Full Length Article

Enhanced optical properties of ZnO nanorods decorated with gold nanoparticles for self cleaning surface enhanced Raman applications

Quoc Khoa Doan[a,b], Manh Hong Nguyen[c], Cong Doanh Sai[c], Van Thanh Pham[c], Hong Hanh Mai[c], Nguyen Hai Pham[c], Thanh Cong Bach[c], Viet Tuyen Nguyen[c,*], Trong Tam Nguyen[d], Khac Hieu Ho[e], Thi Ha Tran[c,f,*]

[a] Division of Computational Physics, Institute for Computational Science, Ton Duc Thang University, Ho Chi Minh City, Viet Nam
[b] Faculty of Electrical and Electronics Engineering, Ton Duc Thang University, Ho Chi Minh City, Viet Nam
[c] Faculty of Physics, VNU University of Science, Vietnam National University, Hanoi, 334 Nguyen Trai, Thanh Xuan, Hanoi, Viet Nam
[d] Department of Physics, Faculty of Basic – Fundamental Sciences, Vietnam Maritime University, 484 Lach Tray – Le Chan, Hai Phong, Viet Nam
[e] Institute of Research and Development, Duy Tan University, 03 Quang Trung, Danang, Viet Nam
[f] Department of Physics, Faculty of Basic Science, University of Mining and Geology, Duc Thang, Tu Liem, Hanoi, Viet Nam

ARTICLE INFO

ABSTRACT

Raman is a very useful tool to identify chemical substances. However, Raman signal is normally not very strong and hence it is important to fabricate surface enhance Raman scattering (SERS) substrates of good repeatability and high enhancement factor. In this study, ZnO nanorods were prepared by a facile hydrothermal process assisted with galvanic effect. Gold nanoparticles were decorated on the as-prepared nanorods by sputtering method. The results showed that the Au nanoparticles enhance photoluminescence, Raman scattering and photocatalyst properties of ZnO nanorods. The ZnO@Au based SERS substrate showed high enhancement factor and can detect methylene blue at low concentration of 10^{-9} M. In combination with self cleaning under UV irradiation, the ZnO@Au SERS substrates can be reusable and hence it is promising for quantitative analyzing based on Raman scattering.

1. Introduction

Since its discovery, Raman spectroscopy has been expected to provide various applications based on characterized Raman signal of chemical substances. In fact, low intensity of Raman signals had limited the applicability of Raman spectroscopy for several decades until the development of surface enhanced Raman scattering (SERS). The very first SERS substrates were rough metallic electrodes [1]. Higher reactive SERS substrates were later fabricated by self assembled layer of noble metal nanoparticles on planar surface [2–5]. The main disadvantage of such substrates is low repeatability, which limits quantitative applicability of Raman technique. Much effort of scientists was devoted to develop new kinds of SERS substrates of higher repeatability for different applications such as: analytical chemistry, biology or environmental science. Recently, 1D nanostructures have been reported as potential SERS substrates of high repeatability and high enhancement factor [6–9]. Even though, localized surface plasmon resesonance in noble metal nanoparticles deposited on such 1D nanostructures is still responsible for SERS activities, higher density of hot spots and effect of

anisotropic geometry are expected to result in better enhancement. Furthermore, core/shell geometry was believed to be able to concentrate the scattering electromagnetic field at the metal surface [10]. The drawback of such approaches is the complicated and/or expensive preparation routes [11].

In fact, most of SERS substrates cannot be reused. This is not beneficial from both economical point of view and quantitative analytical point of view. Hence, preparing of recyclable SERS substrates is very important and has been studied recently. It is well-known that photocatalyst is an effective way to decompose organic materials [12–14]. In this regards, photocatalyst is extremely useful and convenient to clean off chemical substances from used substrates [15–17].

Various ZnO nanostructures such as: nanodisks, nanowires, nanorods, nanopartilces were synthesized by different techniques: microwave, thermal evaporation, hydrothermal method [18–20]. In this study, ZnO nanorods were prepared by hydrothermal method assisted with galvanic effect on cheap print circuit boards (PCBs). Facile synthesis process, cheap precursors and materials are advantageous to scale up the production for commercialization. Galvanic effect helps to

---

improve both density and alignment of ZnO nanorods. This is important to gain better reproducibility of the as-prepared SERS substrates. Instead of using silver which might limit stability of SERS substrate due to oxidation in air, gold nanoparticles with many excellent plasmonic, catalyst properties [21–24], were decorated on surface of ZnO nanorods by sputtering method. Our results show that gold nanoparticles vastly improve photoluminescence, Raman scattering and photocatalyst activity of ZnO nanorods. The combination of these properties makes ZnO:Au nanorod a promising SERS substrate, which possesses high enhancement, reproducibility and can be reusable.

Even though, there were few reports on surface enhanced Raman scattering on semiconductor/noble metal nanocomposites. There is a lack of study on simultaneous enhancement of photoluminescence, Raman scattering and photocatalyst of ZnO@Au nanocomposite. Detailed discussion on the role of gold nanoparticles on enhancement of photoluminescence, surface enhanced Raman scattering, photocatalytic properties of ZnO in this study is expected to contribute to enlighten the relation between these optical properties in ZnO/Au nanorods.

2. Experiment

ZnO nanorods were synthesized on PCBs by galvanic effect assisted hydrothermal method. The detailed experiment setup is described elsewhere [20,25]. In a typical process, PCBs served as substrates were cleaned in sequence with acetone, ethanol and deionized water by ultrasonic bath for 5 min each. The oxide layer on PCB was then removed by HCl solution of 5%, and rinsed thoroughly again with DI water and dried by nitrogen blow. Galvanic cell structure was formed by covering edges of the substrate by Al foils. Then, the as-prepared substrates were transferred into mixture solution of 75 mM zinc nitrate hexahydrate (Zn(NO)$_3$·6H$_2$O) and hexamethylenetetramine (C$_6$H$_{12}$N$_{42}$). Temperature of the whole system was maintained at 90 °C by a temperature controller for hydrothermal reaction and the reaction time was kept at 3 h. ZnO nanorods would be grown in uncovered area of the substrates. Then, the Al cover was removed and the samples were rinsed thoroughly with DI water to get rid of any residual salts from the samples before being blown dried with nitrogen gas.

Gold nanoparticles were decorated onto ZnO nanorods by sputtering method. Different deposition times were applied (from 10 s to 120 s) with a current of 30 mA. X-ray diffractometer Siemens D5005 - Bruker with monochromatized Cu K$_\alpha$ radiation 1.54056 Å was used to characterize structure of the samples. Sample morphology was investigated by using Nova Nano SEM 450. Raman measurement was done on HR 800 Raman spectrometer from Horiba Jobin Yvon. Excitation source was 632.8 nm line from He – Ne laser. Laser power at sample surface was kept at 0.5 mW while acquisition time was 20 s for all the SERS measurement. Diffuse reflectance spectra of ZnO:Au nanorods were collected on Carry 5000 ultraviolet–visible–near infrared (UV–Vis-NIR) spectrophotometer.

Methylene blue (MB) was used as SERS probe molecular in our experiment. Aqueous solution of MB with concentration in the range of 10^{-7} to 10^{-9} were prepared by serial dilution of the initial solution of 10^{-7} M concentration. Self-cleaning cycles of ZnO@Au SERS substrates were performed by wetting the substrate with DI water and shining the sample by UV irradiation from Philips UV lamp in 60 min. After UV irradiation, the samples were then rinsed with DI water, and blown dry by nitrogen gas. The substrate was then ready for being retested with Raman measurement.

3. Results and discussions

Raman spectra of ZnO nanorods prepared by galvanic effect assisted hydrothermal method in 3 h is shown in Fig. 1. Two prominent peaks can be seen in all spectra at 99 and 437 cm^{-1}, corresponding to characteristic Raman modes E$_2^{low}$ and E$_2^{high}$ of ZnO. While E$_2^{low}$ mode is related to vibration of zinc lattice, E$_2^{high}$ is attributed to vibration of
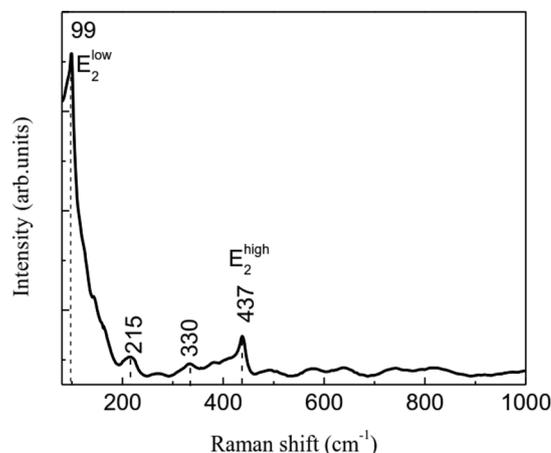
Fig. 1. Raman spectra of ZnO samples prepared by galvanic effect assisted hydrothermal method.

oxygen atom. High intensities of these two peaks imply high crystal quality of the samples. Two weak peaks at 215 and 330 cm^{-1} were reported previously as the second-order Raman scattering arising from zone-boundary phonons (2-TA(M), and 2-E$_2$(M), respectively) [18]. The appearance of these two peaks in the Raman spectra suggests slight oxygen deficiency in our ZnO nanorods.

As can be seen from SEM image in Fig. 2, the as prepared ZnO nanords are quite uniform in size and shape. The rods have diameter of about 200–300 nm and length of up to several micrometers. High density of ZnO nanorods clearly demonstrates the advantage of galvanic effect assisted hydrothermal method in preparation of well aligned nanorods.

XRD patterns of ZnO nanorods shown in Fig. 3 matched well with JSPS card no. 36–1451 of ZnO with hexagonal structure. Lattice parameters of the samples are: a = 0.32 nm; c = 0.52 nm. Crystalline size of nanorods estimated by using Debye Sherrer's formula is 46 nm.

We believe that good alignment and uniformity are critical to enhancement capacity of SERS substrates based on ZnO nanorods. Density of hotspot for enhancement, which is distributed in along arrays of nanorods (3D) is much higher than in the case of planar (2D) distribution. In this regard, higher density of nanorods should result in higher density of hotspots, which in turn offers higher enhancement factor as well as uniformity of SERS substrate. The results showed that the as prepared sample met these criteria for making good SERS substrate. The ZnO nanorod sample prepared in 3 h was then decorated with gold nanoparticles by sputtering methods. Fig. 4 shows TEM
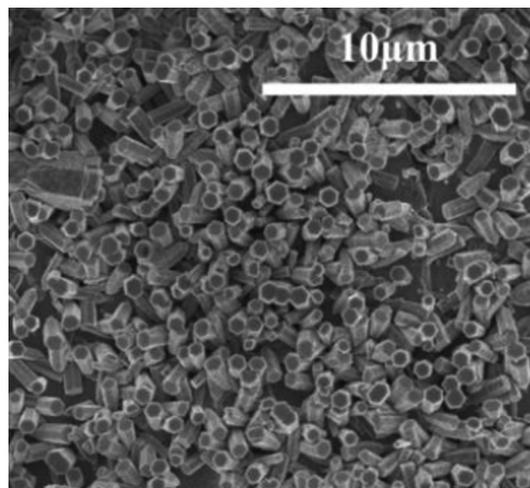
Fig. 2. SEM images of the as prepared ZnO nanorods.
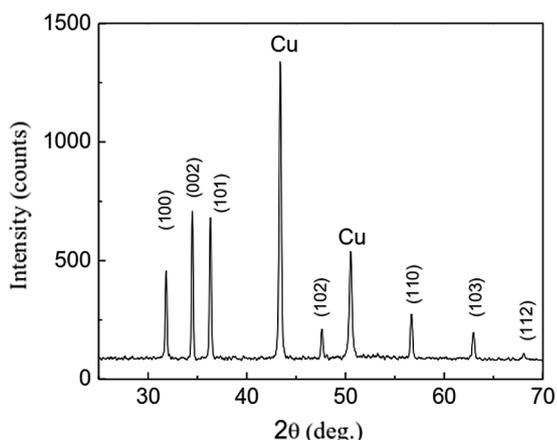
Fig. 3. XRD patterns of ZnO nanorods prepared in 3 h at 90 °C.

images of ZnO nanorods decorated with gold by sputtering method with different sputtering time. Sputtering time of less than 30 s resulted in formation of separated gold nanoparticles on the surface of ZnO nanorods. The size of gold nanoparticles is 10–30 nm. Increasing sputtering times tends to increase size and density of these nanoparticles. At longer sputtering times, some nanoparticles are merged together to form larger island or even continuous layer of gold on ZnO nanorods.

EDS elemental mapping for ZnO nanorods prepared with sputtering time of 30 s was performed. The mapping area is indicated by the rectangle in Fig. 5(a) and the mapping of Au element on the surface of ZnO nanorods is shown in Fig. 5(b). The results help to clarify that gold is distributed in form of nanoparticles on the surface of the nanorods.

Fig. 6 shows typical EDS spectra of ZnO nanorods prepared in 3 h before and after sputtering of gold nanoparticles. EDS measurement reconfirms that the as-prepared ZnO nanorods are pure and clean, no residue or contaminant exists in the final nanoproduct. After 10 s of sputtering, a clear peak of gold appeared in the spectrum. As increasing sputtering time, gold peaks in the EDS spectra become stronger (data not shown).

Diffuse reflectance spectra of ZnO nanorods and ZnO nanorods decorated with gold nanoparticles with different sputtering time 30, 60 and 120 s were measured to investigate localized surface plasmon of ZnO@Au nanorods. The corresponding absorption spectra of the samples, obtained by using Kubelka – Munk function are shown in Fig. 7. Absorption spectrum of ZnO nanorods shows a clear absorption edge at 385 nm corresponding to a band gap of E_g = 3.27 eV.

The absorption spectra of ZnO nanorods before and after decorating with Au nanoparticles show clear difference. In addition to the clear absorption edge of ZnO at around 380 nm, strong absorption peaks at longer wavelengths can be observed. The sample prepared with sputtering time of 30 s shows a clear peak at 532 nm, which is attributed to localized surface plasmon resonance of gold nanoparticles on ZnO nanorods [26]. As increasing sputtering time to 60 s, another notable peak appears at 470 nm while plasmon related peak at 532 nm reduces to a shoulder. At sputtering time of 120 s, plasmon resonant peak becomes much weaker and cannot be resolved. At the same time, absorption peak at 470 nm becomes dominant in the spectra. According to Tapan Barman [27], peak at 470 nm can be attributed to interband absorption of gold nanoparticles. As intraband is far from excitation wavelength used in this measurement (632.8 nm) it might not be useful for surface enhanced Raman scattering. For this reason, we chose sputtering time of 30 s for further investigation of SERS.

The change in photoluminescence of ZnO nanorods under decoration of gold nanoparticles is shown in Fig. 8. It is noted that after deposition of gold, exciton related emission at 380 nm is greatly enhanced while the green emission due to defects like zinc interstitial or oxygen vacancies is much reduced. Upon increasing sputtering time to 60 s, the green broadband is totally suppressed. Several explanations are possible
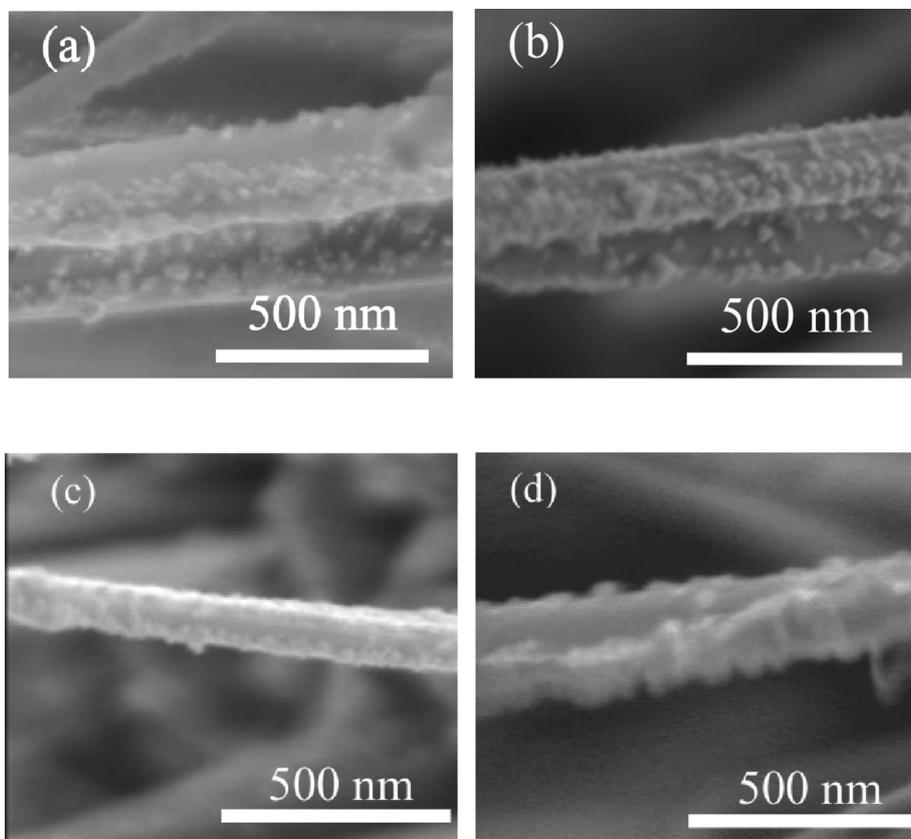
Fig. 4. TEM images of ZnO nanorods decorated with gold at different sputtering time: (a) 10 s; (b) 30 s; (c) 60 s and (d) 120 s.
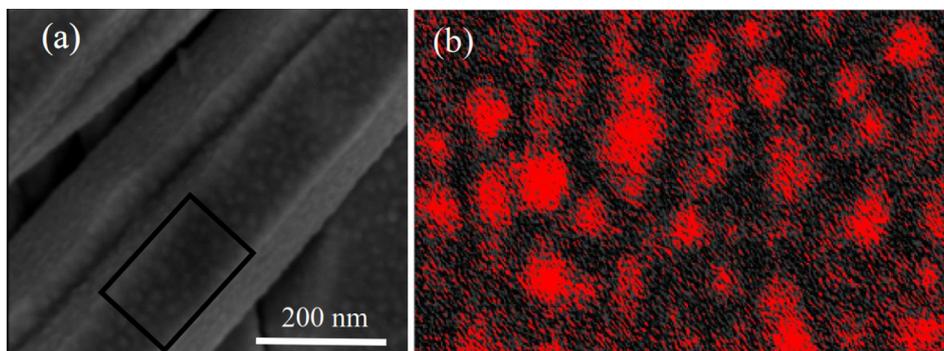
Fig. 5. (a) Enlarged TEM image of ZnO@Au nanocomposite sample prepared with sputtering time of 30 s and (b) EDS mapping of Au element on the surface of ZnO nanorods corresponding to the area marked by black rectangle in (a).

for such phenomenon. First, coating ZnO nanorods with gold may passivate defect and surface states, and results in decreasing the defect peak in ZnO. However, surface passivation is usually reported to reduce partially defect related photoluminescence in ZnO [28,29]. In our case, the green emission is almost impossible to observe even with sample sputtered in only 10 s. Furthermore, along with the decrease of green emission, the increase of excitonic band cannot be explained by taking into account only the trap/surface passivation. It should be understood that other physics phenomenon should be considered. In our opinion, another reason for the observed phenomenon is the coupling between surface plasmon absorption of Au nanoparticles and photoluminescence of ZnO nanorods. Diagram of mechanism for enhancement of band edge emission in ZnO nanorods is illustrated in Fig. 9. Firstly, the emission from trap or surface states of ZnO can easily be absorbed by Au nanoparticles under surface plasmon resonant condition. Such explanation is reasonable when taking into account the closed value of localized surface plasmon wavelength of Au nanoparticles (532 nm) and defect emission from ZnO nanorods in region 500–600 nm. Secondly, band edge emission is also enhanced via charge transfer process, in which electron in defect levels of ZnO is transferred to Fermi level of Au. This process is allowed because defect levels of ZnO is about 5 eV (respect to vacuum level) while Fermi level of gold lies at -5.3 eV [30]. The electron, transferred into Au nanoparticles, can be excited via surface plasmon resonance to energy levels above conduction band of ZnO. In the next step, these excited electrons will be brought back to ZnO conduction band. Hence, along with suppression of defect emission, surface plasmon resonance assisted increment of electron density in conduction band and helped to enhance band edge transition of ZnO nanorods. It should be noted that further increasing sputtering time will not result in more enhancement but rather that excitonic emission becomes saturation and decrease latter. The formation of continuous gold layer on ZnO nanorods might explain for such decrement.

The ZnO@Au nanostructures show high SERS activity, which was demonstrated by clear peaks of MB measured on the as-prepared ZnO@Au nanorods. The SERS spectra of MB on ZnO@Au with different sputtering time are shown in Fig. 10. It can be seen that no Raman signal of MB on bare ZnO nanorods can be detected. On the other hand, clear characteristics peaks of MB are observed when measuring on ZnO@Au substrates, for examples peaks at 1393 cm^{-1}, 1621 cm^{-1}. It is evident that sputtering time plays an important role on enhancement ability.

Even though, Raman enhancement is only slightly different with sputtering time in range of 10–30 s with highest Raman intensity obtained at sputtering times of 30 s. At longer sputtering time 60 s or 120 s, Raman intensity of MB becomes lower. We understand that increasing sputtering time will increase size and density of Au nanoparticles on ZnO nanorods. As the nanoparticles grow larger and at higher density, the probability for the nanoparticles to approach each other at nanometer scale without contact becomes higher. In other words, the increasing number of hot-spots offers higher enhancement. Further increasing sputtering time over 60 s shows only limited enhancement in term of both Raman intensity and number of characteristic Raman peaks. The results show agreement with diffuse reflectance data, which indicate that sample prepared at 30 s showed highest surface plasmon resonance. Sputtering at longer time may eventually result in lower density of hot-spot due to the formation of continuous gold films and weaken surface plasmon resonance as observed in reflectance spectra. It can be concluded that for our investigation, sputtering time of 30 s is optimum for a good SERS activity. It should be noted that SERS enhancement is still available for long sputtering time of 120 s when gold might be in form of thin films on the surface of ZnO nanorods. Lightning rods effect in our ZnO@Au nanorods can be responsible for SERS in this case and hence SERS activity is only faded out but not completely disappeared at longer sputtering time.

SERS spectra of MB at different concentrations on ZnO:Au nanorods were shown in Fig. 11. ZnO@Au nanorods show excellent enhancement ability, which can resolve signal of MB at concentration as low as 10^{-9} M.

The detection limit achieved for ZnO/Au nanorods in this research is comparable with other reports. For example, Huang et al. [15]
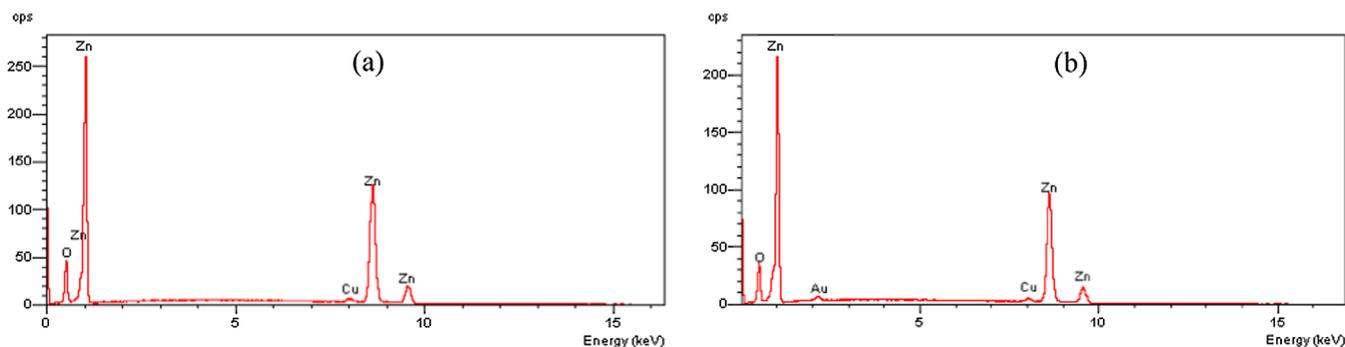
Fig. 6. X-ray energy dispersive spectra of ZnO nanorods prepared in 3 h and ZnO@Au nanorods with sputtering time of 10 s.
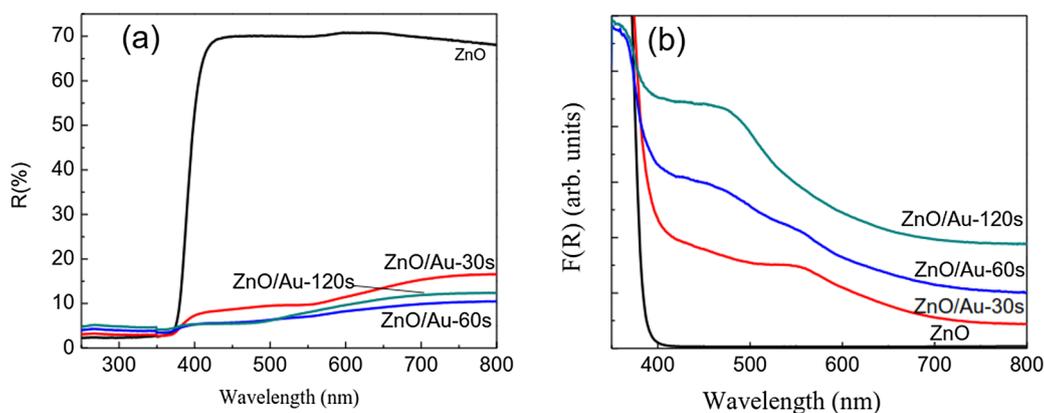
Fig. 7. (a) Diffuse reflectance spectra of ZnO and ZnO@Au nanorods with different sputtering time, (b) the corresponding absorption spectra of ZnO and ZnO@Au nanorods with different sputtering time.
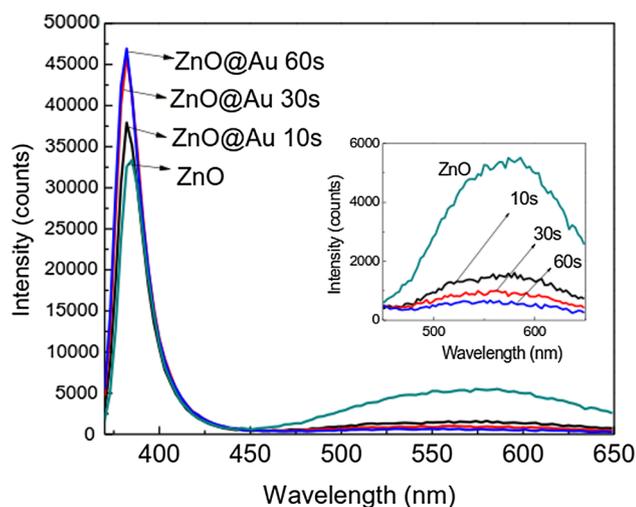
Fig. 8. Photoluminescence of ZnO@Au nanorods prepared with different sputtering time.
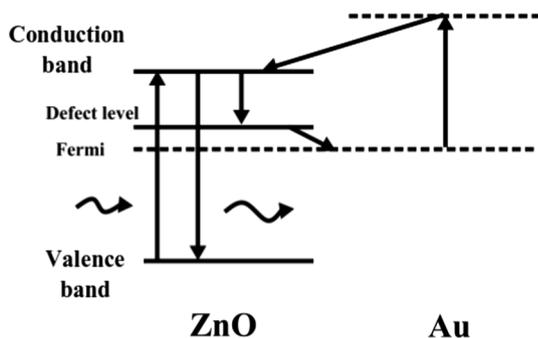
Fig. 9. Diagram of mechanism for enhancement of band edge emission in ZnO nanorods.

Fig. 10. Raman spectra of MB (10^{-7} M) on ZnO@Au nanorods prepared with different sputtering time.
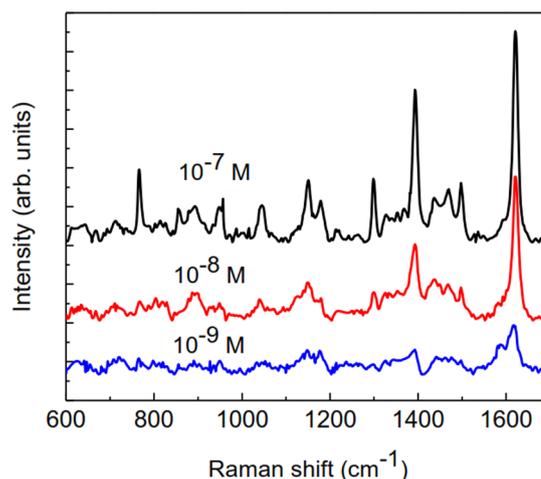
Fig. 11. Raman spectra of MB at different concentration measured on ZnO/Au with sputtering time of 30 s.

reported of using ZnO/Ag multipods to detect Rhodamine B at concentration as low as 10^{-8} M. Sakano et. al [31] also used Au coated ZnO nanorods as SERS substrate to detect RhB with detection limit of 10^{-9} M. Using ZnO/Au nanorods, Nampueng et al. was able to get signal of MB at lowest concentration of 10^{-7} M [32].

Eventhough, the alignment of ZnO/Au nanorods is not totally perfect, the as-prepared substrates show excellent uniformity. This can be understood as the distribution of gold nanoparticles decorated along ZnO nanorods helps to enhance the number of hot–spots greatly when compared with the distribution of gold nanoparticles on 2D flat surface such as Si or sodalime glass substrate. Size of gold nanoparticles on ZnO

nanorods is about 10–30 nm which is much smaller than the excitation laser beam size (~μm). Rough estimation shows that when laser beam hits the surface samples, it excited simultaneously several ZnO nanorods. These nanorods are micrometers in length and can accommodate hundreds of gold nanoparticles along these nanorods. These factors explain for the high enhancement and uniformity of these SERS substrates.
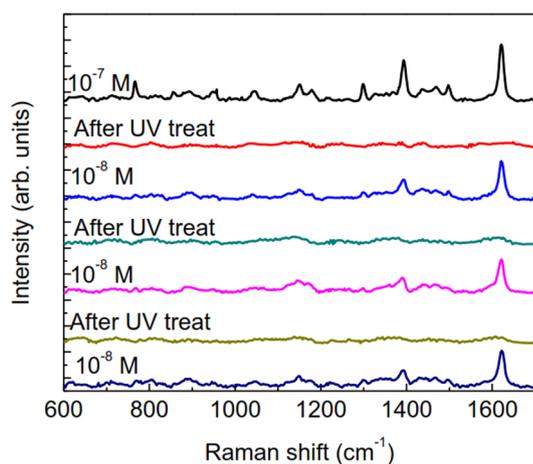
Fig. 12. Raman spectra of MB on ZnO@Au nanorods during adsorption/cleaning cycles.

ZnO@Au nanorods also exibit high photocatalytic activity, which can be taken advantages to make recyclable SERS platform. In addition to economical benefit, recycle ability also offers other advantages such as quantitative analysis or comparing cross section scattering area of various molecular on one common SERS substrate. Fig. 12 shows that ZnO@Au nanorods can be reused after measurement by being exposed under UV irradiation. Raman signal is well reproduced after each self cleaning cycle. It has been reported that SERS substrates based on silver nanoparticles are difficult to be reused due to easy oxidation of silver to silver oxide. The recyclable ability of our samples is resulted from the combination of excellent photocatalyst of ZnO nanorods, which helps to effectively remove organic molecular from the substrate and the chemical stability of both ZnO nanorods and Au nanoparticles, which guarantees to reproduce Raman signal after being cleaned. Under exposure to UV irradiation, electron hole pairs are created. On the surface of ZnO nanorods, electrons and holes react with oxygen and water vapor to produce active group such as: *OH and *O_2. These groups are able to decompose organic compound into CO_2 and H_2O [33]. High surface area of nanorods improves photocatalyst reaction rate. In addition, photocatalyst of ZnO@(Ag,Au) is believed to be even better than pure ZnO nanorods as discussed other reports [34–36]. The better photocatalyst is resulted from the charge transfer from ZnO nanorods to gold nanoparticles, which reduces recombination not being useful for photocatalytic activity.

4. Conclusion

ZnO@Au nanorods were successfully prepared by combination of a facile hydrothermal method assisted with galvanic effect and sputtering method. Decorating Au nanoparticles on ZnO nanorods helps to enhance photoluminescence and surface enhance Raman scattering. The high surface area of nanorods offers several major benefits. First, it helps to maximize both the number of hot spots created by Au nanoparticles decorated on ZnO nanorods, which is necessary for Raman scattering enhancement. Second, high surface to volume ratio is also beneficial for photocatalytic properties.

Simultaneous enhancement of these optical properties offers a kind of SERS substrate of high enhancement factor, high uniformity, with self cleaning effect, which helps to recycle the substrate and opens the ability for quantitative study of substances at low concentrations based on Raman measurement.

Declaration of Competing Interest

The author would like to declare that we have no conflict of interests

References

[1] M. Fleischmann, P.J. Hendra, A.J. McQuillan, Raman spectra of pyridine adsorbed at a silver electrode, Chem. Phys. Lett. 26 (1974) 163–166, https://doi.org/10.1016/0009-2614(74)85388-1.

[2] P. Mosier-Boss, Review of SERS substrates for chemical sensing, Nanomaterials. 7 (2017) 142, https://doi.org/10.3390/nano7060142.

[3] G. Yang, J. Nanda, B. Wang, G. Chen, D.T. Hallinan, Self-assembly of large gold nanoparticles for surface-enhanced raman spectroscopy, ACS Appl. Mater. Interf. 9 (2017) 13457–13470, https://doi.org/10.1021/acsami.7b01121.

[4] K. Kim, L.K. Kyung, H.B. Lee, S.S. Kuan, Surface-enhanced raman scattering on aggregates of silver nanoparticles with, J. Phys. Chem. C. 114 (2010) 18679–18685.

[5] M. Muniz-Miranda, C. Gellini, E. Giorgetti, Surface-enhanced Raman scattering from copper nanoparticles obtained by laser ablation, J. Phys. Chem. C. 115 (2011) 5021–5027, https://doi.org/10.1021/jp1086027.

[6] Y. Li, J. Dykes, T. Gilliam, N. Chopra, A new heterostructured SERS substrate: Free-standing silicon nanowires decorated with graphene-encapsulated gold nanoparticles, Nanoscale 9 (2017) 5263–5272, https://doi.org/10.1039/c6nr09896g.

[7] R. Lu, J. Sha, W. Xia, Y. Fang, L. Gu, Y. Wang, A 3D-SERS substrate with high stability: silicon nanowire arrays decorated by silver nanoparticles, CrystEngComm. 15 (2013) 6207, https://doi.org/10.1039/c3ce40788h.

[8] M. Balamurugan, J. Yang, Three-dimensional surface-enhanced raman scattering substrate fabricated using chemical decoration of silver nanoparticles on electrospun polycarbonate nanofibers, Appl. Spectrosc. 71 (2017) 879–887, https://doi.org/10.1177/0003702816658670.

[9] E. Satheeshkumar, J. Yang, Photochemical decoration of silver nanoparticles on ZnO nanowires as a three-dimensional substrate for surface-enhanced Raman scattering measurement, J. Raman Spectrosc. 45 (2014) 407–413, https://doi.org/10.1002/jrs.4477.

[10] H. Qi, D. Alexson, O. Glembocki, S.M. Prokes, Plasmonic coupling on dielectric nanowire core-metal sheath composites, Nanotechnology 21 (2010), https://doi.org/10.1088/0957-4484/21/8/085705.

[11] D. Li, D.W. Li, Y. Li, J.S. Fossey, Y.T. Long, Cyclic electroplating and stripping of silver on Au@SiO2 core/shell nanoparticles for sensitive and recyclable substrate of surface-enhanced Raman scattering, J. Mater. Chem. 20 (2010) 3688–3693, https://doi.org/10.1039/b924865j.

[12] H. Yi, M. Yan, D. Huang, G. Zeng, C. Lai, M. Li, X. Huo, L. Qin, S. Liu, X. Liu, B. Li, H. Wang, M. Shen, Y. Fu, X. Guo, Synergistic effect of artificial enzyme and 2D nano-structured Bi2WO6 for eco-friendly and efficient biomimetic photocatalysis, Appl. Catal. B Environ. (2019) 52–62, https://doi.org/10.1016/j.apcatb.2019.03.008.

[13] H. Yi, M. Jiang, D. Huang, G. Zeng, C. Lai, L. Qin, C. Zhou, B. Li, X. Liu, M. Cheng, W. Xue, P. Xu, C. Zhang, Advanced photocatalytic Fenton-like process over bio-mimetic hemin-Bi2WO6 with enhanced pH, J. Taiwan Inst. Chem. Eng. 93 (2018) 184–192, https://doi.org/10.1016/j.jtice.2018.06.037.

[14] Y. Yang, C. Zhang, D. Huang, G. Zeng, J. Huang, C. Lai, C. Zhou, W. Wang, H. Guo, W. Xue, R. Deng, M. Cheng, W. Xiong, Boron nitride quantum dots decorated ultrathin porous g-C3 N4: Intensified exciton dissociation and charge transfer for promoting visible-light-driven molecular oxygen activation, Appl. Catal. B Environ. (2019) 87–99, https://doi.org/10.1016/j.apcatb.2018.12.049.

[15] Q. Huang, J. Li, Enhanced photocatalytic and SERS properties of ZnO/Ag hierarchical multipods-shaped nanocomposites, Mater. Lett. 204 (2017) 85–88, https://doi.org/10.1016/j.matlet.2017.06.019.

[16] A.E. Kandjani, M. Mohammadtaheri, A. Thakkar, S.K. Bhargava, V. Bansal, Zinc oxide/silver nanoarrays as reusable SERS substrates with controllable "hot-spots" for highly reproducible molecular sensing, J. Colloid Interf. Sci. 436 (2014) 251–257, https://doi.org/10.1016/j.jcis.2014.09.017.

[17] G. Sinha, L.E. Depero, I. Alessandri, Recyclable SERS substrates based on Au-Coated ZnO nanorods, ACS Appl. Mater. Interf. 3 (2011) 2557–2563, https://doi.org/10.1021/am200396n.

[18] N.V. Tuyen, N.N. Long, T.T.Q. Hoa, N.X. Nghia, D.H. Chi, K. Higashimine, T. Mitani, T.D. Canh, Indium-doped zinc oxide nanometre thick disks synthesised by a vapour-phase transport process, J. Exp. Nanosci. 4 (2009) 243–252, https://doi.org/10.1080/17458080802627482.

[19] T.D. Canh, N.V. Tuyen, N.N. Long, Influence of solvents on the growth of zinc oxide nanoparticles fabricated by microwave irradiation, VNU J. Sci.: Math.-Phys. 25 (2009) 71–76.

[20] H.H. Mai, V.T. Pham, V.T. Nguyen, C.D. Sai, C.H. Hoang, T.B. Nguyen, Non-enzymatic fluorescent biosensor for glucose sensing based on ZnO Nanorods, J. Electron. Mater. 46 (2017), https://doi.org/10.1007/s11664-017-5300-8.

[21] L. Qin, G. Zeng, C. Lai, D. Huang, C. Zhang, P. Xu, T. Hu, X. Liu, M. Cheng, Y. Liu, L. Hu, Y. Zhou, A visual application of gold nanoparticles: Simple, reliable and sensitive detection of kanamycin based on hydrogen-bonding recognition, Sensors Actuat. B Chem. 243 (2017) 946–954, https://doi.org/10.1016/j.snb.2016.12.086.

[22] W. Rao, D. Wang, T. Kups, E. Baradács, B. Parditka, Z. Erdélyi, P. Schaaf, Nanoporous gold nanoparticles and Au/Al2O3 hybrid nanoparticles with large tunability of plasmonic properties, ACS Appl. Mater. Interf. 9 (2017) 6273–6281, https://doi.org/10.1021/acsami.6b13602.

[23] D. Wang, R. Ji, P. Schaaf, Formation of precise 2D Au particle arrays via thermally

induced dewetting on pre-patterned substrates, Beilstein J. Nanotechnol. 2 (2011) 318–326, https://doi.org/10.3762/bjnano.2.37.

[24] D. Wang, P. Schaaf, Nanoporous gold nanoparticles, J. Mater. Chem. 22 (2012) 5344–5348, https://doi.org/10.1039/c2jm15727f.

[25] P. Van Thanh, L.T.Q. Nhu, H.H. Mai, N.V. Tuyen, S.C. Doanh, N.C. Viet, D.T. Kien, Zinc oxide nanorods grown on printed circuit board for extended-gate field-effect transistor pH sensor, J. Electron. Mater. 46 (2017) 3732–3737, https://doi.org/10.1007/s11664-017-5369-0.

[26] A. Vincenzo, P. Roberto, F. Marco, M.M. Onofrio, I. Maria Antonia, Surface plasmon resonance in gold nanoparticles: a review, J. Phys. Condens. Matter. 29 (2017) 203002 http://stacks.iop.org/0953-8984/29/i=20/a=203002.

[27] T. Barman, A.A. Hussain, B. Sharma, A.R. Pal, Plasmonic hot hole generation by interband transition in gold-polyaniline, Sci. Rep. 5 (2015) 1–5, https://doi.org/10.1038/srep18276.

[28] J.P. Richters, T. Voss, D.S. Kim, R. Scholz, M. Zacharias, Enhanced surface-excitonic emission in ZnO/Al$_2$O$_3$ core-shell nanowires, Nanotechnology 19 (2008), https://doi.org/10.1088/0957-4484/19/30/305202.

[29] C. Chen, H. He, Y. Lu, K. Wu, Z. Ye, Surface passivation effect on the photoluminescence of ZnO nanorods, ACS Appl. Mater. Interf. 5 (2013) 6354–6359, https://doi.org/10.1021/am401418b.

[30] C.W. Cheng, E.J. Sie, B. Liu, C.H.A. Huan, T.C. Sum, H.D. Sun, H.J. Fan, Surface plasmon enhanced band edge luminescence of ZnO nanorods by capping Au nanoparticles, Appl. Phys. Lett. 96 (2010) 1–4, https://doi.org/10.1063/1.3323091.

[31] T. Sakano, Y. Tanaka, R. Nishimura, N.N. Nedyalkov, P.A. Atanasov, T. Saiki, M. Obara, Surface enhanced Raman scattering properties using Au-coated ZnO nanorods grown by two-step, off-axis pulsed laser deposition, J. Phys. D. Appl. Phys. 41 (2008), https://doi.org/10.1088/0022-3727/41/23/235304.

[32] N. Pangpaiboon, T. Amsiri, S. Kalasung, C. Chananonnawathorn, V. Patthanasettakul, M. Horprathum, N. Nuntawong, S. Limwichean, P. Eiamchai, Controllable decoration of Au NPs on zinc oxide nanorods template by magnetron sputtering technique for reusable-SERS active surface enhancement, AIP Conf. Proc. 2010 (2018), https://doi.org/10.1063/1.5053199.

[33] X. Chen, Z. Wu, D. Liu, Z. Gao, Preparation of ZnO photocatalyst for the efficient and rapid photocatalytic degradation of Azo dyes, Nanoscale Res. Lett. 12 (2017) 4–13, https://doi.org/10.1186/s11671-017-1904-4.

[34] A.A. El-Bindary, S.M. El-Marsafy, A.A. El-Maddah, Enhancement of the photocatalytic activity of ZnO nanoparticles by silver doping for the degradation of AY99 contaminants, J. Mol. Struct. 1191 (2019) 76–84, https://doi.org/10.1016/j.molstruc.2019.04.064.

[35] P. Li, Z. Wei, T. Wu, Q. Peng, Y. Li, Au−ZnO hybrid nanopyramids and their photocatalytic properties, J. Am. Chem. Soc. 133 (2011) 5660–5663.

[36] I. Unlu, J.W. Soares, D.M. Steeves, J.E. Whitten, Photocatalytic activity and fluorescence of Gold/Zinc oxide nanoparticles formed by dithiol linking, Langmuir 31 (2015) 8718–8725, https://doi.org/10.1021/acs.langmuir.5b01632.